UDK 620.1:620.193:620.194.2:621.643.2-034.14
Original scientific article/Izvirni znanstveni članek

ISSN 1580-2949
MTAEC9, 53(1)81(2019)

STRESS-CORROSION-CRACKING ASSESSMENT OF X52 PIPELINE STEEL EXPOSED TO MEXICAN SOILS

OCENA POKANJA ZARADI NAPETOSTNE KOROZIJE NA CEVOVODU IZ JEKLA X52, IZPOSTAVLJENEMU MEHIŠKI PRSTI

Carlos Rafael Lizárraga[1], Tezozomoc Pérez[2], Ricardo Galván-Martinez[3], Luis Manuel Quej-Aké[4], Antonio Contreras[4*]

[1]Department of Metal-Mechanics, National Technological Institute of Mexico – Technological Institute of Culiacán, Juan de Dios Bátiz 310, Pte. Col. Guadalupe, 80220 Culiacán, Sinaloa, México
[2]Corrosion Research Centre, Autonomous University of Campeche, Ave. Agustín Melgar s/n, Col Buenavista, P.O. Box 24039, Campeche, México
[3]Anticorrosion Unit, Engineering Institute, University of Veracruz, Juan Pablo II s/n, University Zone, C.P. 94294, Boca del Río, Veracruz, México
[4]Mexican Petroleum Institute, Eje Central Lázaro Cárdenas Norte 152, Col. San Bartolo Atepehuacan, 07730 México City, México

Prejem rokopisa – received: 2018-02-07; sprejem za objavo – accepted for publication: 2018-10-10

doi:10.17222/mit.2018.018

This work analyzed the physicochemical effect of the soils typical of the Campeche State of Mexico on the X52 pipeline steel. The susceptibility to external stress corrosion cracking (SCC) of the X52 pipeline steel in two types of soil containing different moisture contents was investigated using slow-strain-rate tests (SSRT). One soil is of a calcareous origin (high pH) and the other is farming soil (near-neutral pH). Generally, steel shows high resistance to SCC in the farming soil, exhibiting only pitting corrosion; however, the X52 steel was susceptible to SCC, though only in the saturated calcareous soil, showing some microcracks in the gage section of SSR specimens. Some microcracks were found at the bottom of micropits. SCC was promoted by the plastic deformation at the bottom of the pits, combined with the influence of the soil chemistry. The process of crack initiation is discussed in terms of the pit geometry and stresses.

Keywords: corrosion, soil, pitting, stress corrosion cracking

Avtorji so analizirali fizikalno-kemijski vpliv prsti, značilne za mehiško državo Campeche, na cevovod iz jekla X52. Občutljivost cevovoda iz jekla X52 na korozijsko pokanje zaradi zunanjih napetosti (SCC) so raziskovali na dveh vrstah različno vlažne prsti z uporabo testov počasne deformacije (SSRT). Ena prst je bila apnenčastega izvora (visok pH) in druga je bila poljedelska zemlja (blizu nevtralnega pH). V splošnem se je pokazalo, da ima jeklo dobro odpornost proti SCC v poljedelski zemlji z rahlimi znaki jamičaste korozije. Vendar pa jeklo X52 kaže večjo občutljivost na SCC v prisotnosti nasičene apnenčaste prsti z znaki nastajanja mikrorazpok v merilnem delu SSR preizkušancev. Nekaj mikrorazpok so našli tudi na dnu jamic. SCC je pospešila plastična deformacija na dnu jamic v kombinaciji z vplivom kemijske sestave prsti. Proces nastajanja razpok so avtorji razložili glede na geometrijo jamic in napetosti.

Ključne besede: korozija, prst, nastajanje jamic, pokanje zaradi napetostne korozije

1 INTRODUCTION

Research in the external-stress corrosion cracking (SCC) of pipelines caused by the soils is currently of great interest in the oil industry. SCC of underground pipelines can develop in a few years, depending on the operating conditions. SCC is a type of environmentally assisted cracking that requires three factors in order to occur: the mechanical factor, the metallurgical factor and the electrochemical factor.

Currently, in México, SCC is beginning to be a problem in the oil industry because several SCC cases were detected through smart pigs, preventing the occurrence of a failure to the pipeline.[1] Most SCC studies focused on the pipelines of low-carbon steels, taking into account the internal fluid that is transported, mainly H_2S and CO_2.[2–5] However, when a pipeline is designed, in addition to the internal fluid that is being transported, the external environment (soil-water) must also be considered.[6–7]

The investigation about the pipelines that has developed includes a wide range of diameters, wall thicknesses, grades, manufacturing processes and coatings.[8] The relationship between the pipelines and SCC is not clear due to many factors that must be considered, such as the environment (the type of soil), stresses, the chemical composition of steel, the grade, strength and microstructure of pipeline steel. The factors that must be considered when dealing with the SCC produced due to the external environment include the moisture content, pH, temperature, the concentration of dissolved ions, carbonate amount, the level of cathodic protection, the microstructure of pipeline steel and operational and residuals stresses.[7,9]

When cracks nucleate in the surface of a pipeline, the conditions allowing them to reach the critical size

*Corresponding author e-mail:
acontrer@imp.mx

depend on several parameters such as the corrosiveness of the environment (physicochemical factors commonly associated with pH), the microstructure of steel (associated with the phases present in the material, grain size, inclusions and others defects) and mechanical factors (the material strength, the stress applied, fluctuations of the pressure and residual stresses).

Most of the works about the SCC of pipeline steels were done using synthetic solutions representative of some specific geographical areas.[10–11] Mexico is a country with a wide variety of soils and climates. Therefore, in this work we used two different soils from the south of Mexico where there is a great number of underground pipelines that transport oil, focusing on how the environment and the stresses produced by slow strain affect the nucleation of cracks on the steel surface. Ion content, pH, moisture amount and phases are some of the soil parameters that we have studied.

2 EXPERIMENTAL PART

2.1 SCC assessment

The SCC in the X52 steel was evaluated through SSR tests. SSRT specimens used to evaluate the SCC susceptibility were machined from the X52 pipeline steel (914 mm in diameter and 9.5 mm in thickness) according to the measurements indicated in NACE TM 0198.[12]

The SSRT specimens were exposed to two different soils obtained from the south of México. One type of soil is of calcareous origin (pH 8.5) and the other is farming soil (pH 6.5). The soil samples used for the experiments were prepared at a controlled water content, corresponding to (25, 50 and 100) % of the saturation level.

To perform the SSR tests involving the two different soils, a 500-mL glass autoclave was used as shown in **Figure 1**. A mobile constant-extension-rate machine – MCERT – (**Figure 1a**) with a load capacity of 44 kN was used to perform the SSRT at a strain rate of $1 \cdot 10^{-6}$ s^{-1}. The tests were carried out in air as reference (**Figure 1b**) and in the two soils with different moisture contents (25, 50 and 100) % at room temperature. When a test was completed, the fractured sample was immediately removed and cleaned using acid and acetone for an examination with scanning electron microscopy (SEM).

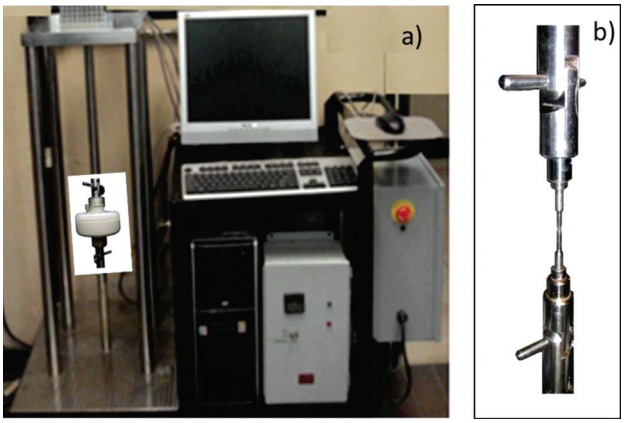

Figure 1: a) MCERT machine used to carry out the SSR tests consisting of a glass cell with calcareous soil and b) SSRT carried out in air

The SCC susceptibility was evaluated according to NACE TM-0198 and ASTM G-129.[12,13] An SCC index higher than 0.8 means that the material exhibits good resistance to SCC, whereas lower values (<0.8) indicate that the material evaluated may be susceptible to SCC. In this case, complementary SEM observations are required to confirm the presence of cracks. These observations are recommended when there is a ratio lower than 0.8.

3 RESULTS AND DISCUSSION

3.1 Steel microstructure

The microstructure of the API X52 steel consists of perlite and ferrite. The average grain size of this steel is around 10 μm. Several recent studies of steels with different microstructures have suggested that steels with more uniform microstructures may be less susceptible to SCC.[14,15] Investigations of steel revealed that the microstructure is the most important factor affecting SCC.[14–18] Therefore, in addition to steel grade, the microstructure also needs to be considered when determining the SCC susceptibility.

3.2 Soil analysis

Table 1 shows the chemical compositions of the soils used. In the calcareous soil, the main constituent is calcium, forming a higher amount of carbonates than the one found in the farming soil as shown in **Table 2.**

Table 1: Chemical compositions of the soils studied (*w*/%)

Metals and oxides	Farming soil	Calcareous soil
Na	0.07375	0.003845
Ca	2.47	39.1
Mg	0.54630	0.07661
Fe	3.95	0.02088
Cu	0.001999	ND
Si	0.0536.7	0.04053
Al	9.46	0.02587
K	1.17	0.00532
Cl	0.08	0.59
SiO_2	0.66	35.75
Al_2O3	0.47	25.25
Fe_2O_3	0.12	16.35
CaO	98.57	11.75
MgO	ND	3.99
TiO_2	ND	1.95
P_2O_5	ND	0.52
MnO	ND	0.48
SO_3	0.04	0.41

ND=Not detected

Generally, farming soils are clay compounds with a high organic-matter content as shown in **Table 2.** Farm-

Table 2: Physicochemical parameters of the soils relating to corrosion and SCC

Soil	Resistivity (Ohm·cm)	pH	Redox potential (mV vs SHE)	Organic matter	Moisture content	CO_3^{2-}	HCO_3^-	Cl^-	NO_2^-	NO_3^-	SO_4^{2-}
						(ppm)					
Farm.	3402	6.7	379	11.6 %	43.08 %	111.6	63.44	0.90	2.59	9.23	6.59
Calc.	13417	8.1	335	3.23 %	22.52 %	120	597.8	0.52	2.21	1.56	1.00

Table 3: SCC assessment obtained with the SSRTs

	Condition	RA (%)	**RAR**	TF	**TFR**	PE	**PER**	EL	**ELR**	ε	εR
Air	Air	78.59		55.78		17.82		4.85		19.10	
Calcareous soil	25%	52.13	0.66	52.97	0.95	17.11	0.96	4.60	0.95	18.11	0.94
	50%	54.34	0.69	50	0.90	16.78	0.94	4.36	0.89	17.19	0.90
	100%	59.81	0.76	40.77	0.73	12.72	0.71	3.55	0.73	13.98	0.73
Farming soil	50%	56.25	0.71	52.58	0.94	16.74	0.94	4.57	0.94	17.98	0.94
	100%	77.05	0.98	48.98	0.88	15.68	0.88	4.26	0.88	16.77	0.87

ing soils have a notable plasticity when they are wet and they can easily adhere to surfaces. When this soil dries, cracks and stresses occur and these can damage the coating.[19] Pipelines in the soils that experience different periods of high or low moisture are more susceptible to SCC.[20]

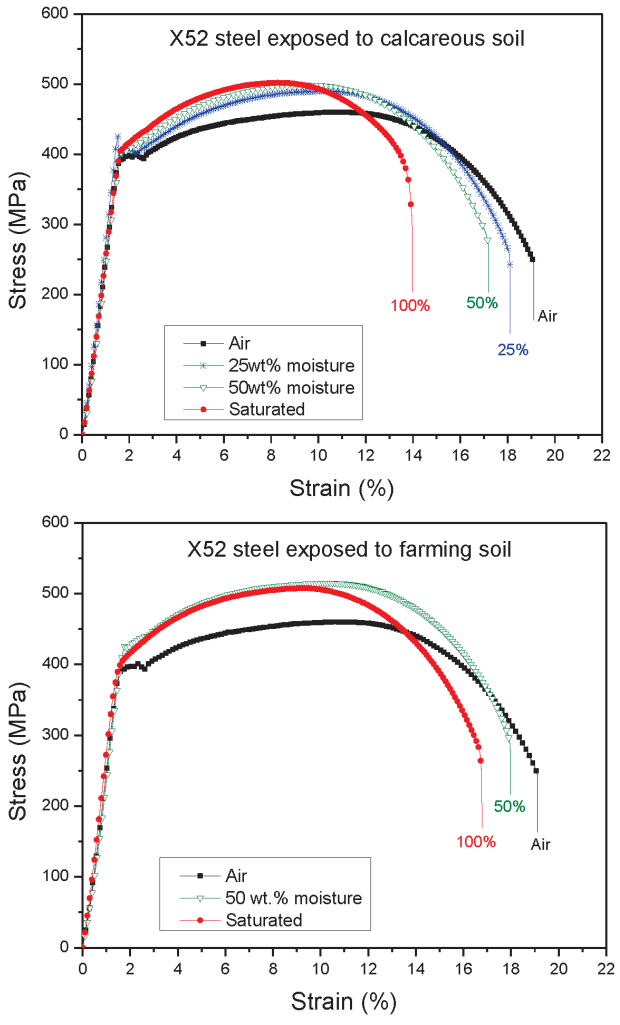

Figure 2: Stress-strain profiles obtained with the SSRTs

Samples of the soils were analyzed with X-Ray diffraction (XRD). The calcareous soil is basically composed of calcium carbonate ($CaCO_3$-Calcite) and some traces of silicon oxide (SiO_2-Coesite) and iron oxide (Fe_3O_4). The farming soil basically includes aluminum-silicate-oxide (Al_2SiO_5), aluminum oxide (Al_2O_3), silicon oxide (SiO_2), iron oxides (Fe_3O_4) and some traces of phosphorus and titanium oxides.

3.3 Slow-strain-rate tests

Figure 2 shows the stress-strain curves obtained with the SSRTs carried out in air and in the soils with different moisture contents at room temperature. According to this figure, it is clear that the strain decreases as the moisture content increases, which can be attributed to the dissolution of salts and ions increasing the corrosivity of the SSR samples due to the soils. The mechanical properties of the X52 steel obtained with the SSRT tests include a yield strength of 398 MPa, an ultimate tensile strength of 460 MPa, a 19-% strain and an elongation of 4.85 mm.

3.4 Assessment of SCC susceptibility

Susceptibility to SCC of the API X52 steel was evaluated on the basis of the results obtained with the SSRTs and corroborated with the SEM observations. **Table 3** shows a summary of the SCC assessment obtained with the SSRTs. The SCC susceptibility was expressed as a function of the reduction in area ratio (RAR), time-to-failure ratio (TFR), plastic-elongation ratio (PER), elongation ratio (ELR) and strain ratio (εR).[12,13] Ratios higher than 0.8 normally indicate good SCC resistance, whereas the values lower than 0.8 indicate susceptibility to SCC, which should be corroborated with SEM.

The SCC index showed in **Table 3** indicates that the X52 steel is resistant to SCC, except when the X52 steel is exposed to saturated calcareous soil where all the SCC indices calculated were below 0.8, indicating that steel may be susceptible to SCC in this soil, which was corroborated with the SEM observations.

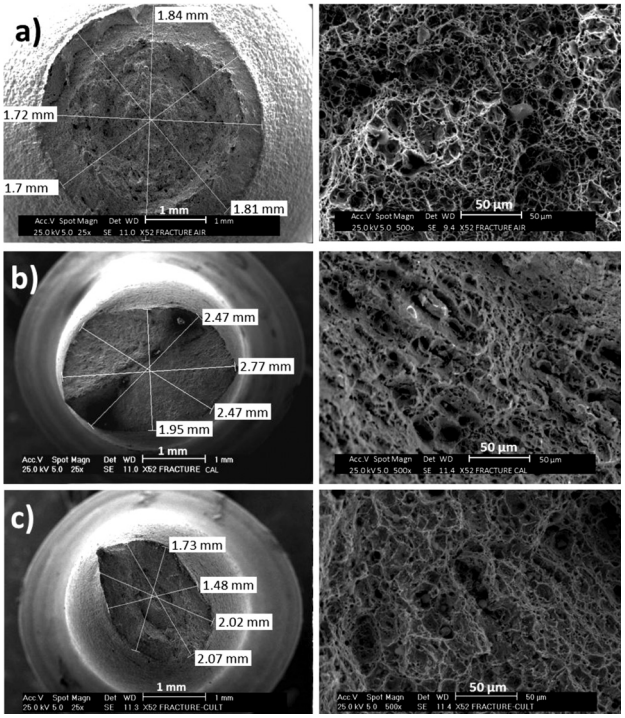

Figure 3: SEM images of the fracture surfaces: a) tested in air, b) tested in saturated calcareous soil and c) tested in saturated farming soil

3.5 Surface-fracture analysis

Figure 3 shows SEM images of the fracture surfaces (primary cracks) of the steels after the SSRTs were carried out in air and in both calcareous and farming soils. The measurements of the final diameters of the fractures needed to calculate the RARs were carried out. For most of the samples tested with both soils, a ductile type of fracture was observed, except for the samples tested in the saturated calcareous soil where a brittle fracture was observed (**Figure 3b**).

The surface fractures showed some inclusions like MnS, SiO_2, Al_2O_3 and FeC. The pit formation at these sites may have been enhanced by the galvanic coupling between the inclusions and the base metal. Inclusions enriched in Al_2O_3 and SiO_2 are hard and brittle. According to Liu et al.,[16] inclusions act as crack-initiation sites. Zorc et al.[21] said that cracks are directly connected to the non-metallic inclusions of the oxide types.

3.6 Longitudinal-section analysis

The SEM analysis was focused on the sections of the SSRT specimens exposed to the saturated calcareous soil where the SCC assessment gave a SCC index below 0.8. **Figure 4** shows SEM images of the longitudinal sections of the samples tested in the saturated calcareous soil, showing the presence of some typical secondary cracks and pits close to the surface failure (the primary crack). **Figure 4a** shows a lateral view of the primary crack of the fracture surface. The appearance of the surface fracture is typical of brittle fracture. **Figure 4b** shows the presence of some secondary cracks in the gage section close to the primary crack. Such cracks are generally initiated at the pits on the gage surface as shown in **Figures 4c–4d.** However, not all the pits were associated with microcracks. For the samples tested in the calcareous soil with a 50-% moisture content as well as for the samples tested in the farming soil, no secondary cracks were observed.

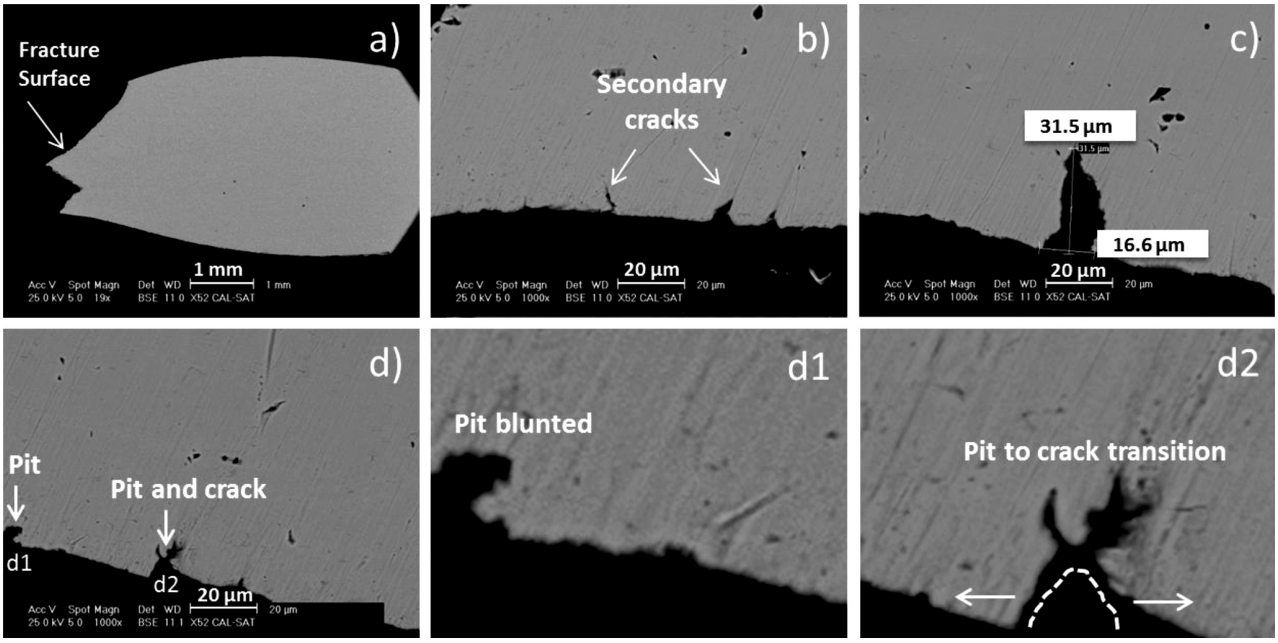

Figure 4: SEM images of the longitudinal sections of the samples tested in the saturated calcareous soil: a) a primary crack, b) secondary cracks close to the surface failure, c) crack measurement and d) some pits and cracks close to the surface failure

From the specimens metallographically prepared, it was observed that most of the cracks were shallow with a depth of a few microns and that they tended to be dormant. Once these shallow cracks reached a threshold depth, they could propagate. The maximum crack depth measured was 31.5 μm and the maximum width was 16.6 μm (**Figure 4c**); the aspect ratio was 1.8, resulting in a high susceptibility to cracking. According to Fang et al.,[22] pits are less likely to generate cracks if the depth-to-width aspect ratio is >0.5. Considering the elapsed time for this test (>40h), we obtained a cracking velocity of 2.14×10^{-4} μm/sec (6.7 mm/year). This cracking velocity is called the pseudo-cracking velocity due to the unknown time, at which the cracks initiate in a specimen during a SSR test. This assumption presumes that a crack starts at the time of the test; a more accurate time of initiation would probably indicate a higher cracking velocity because most of the cracks nucleate due to the yield strength. Thus, the plastic zone is considered to be controlling variable for the threshold stress for the crack nucleation and propagation.[23]

3.7. Transition from a pit to a crack

An SCC process starts with the nucleation of cracks, which, in most cases, initiate from the bottom of a pit due to a combination of an electrochemical process (dissolution) and mechanical process (tensile stress) as shown in **Figure 4d2**.

When an SSRT is being performed, the corrosive environment generates pits and these, in turn, increase the local stresses with a plastic deformation, producing plastic zones in the boundary corrosion pits.[24,25] The pits observed at the high-stress regime may cause incubation and nucleation of cracks.

Depending on the width and depth, a pit can raise the threshold stress at the bottom, usually leading to a crack initiation. This behavior was shown by Hoeppner[26] (Equation 1):

$$K_{\mathrm{fs}} = 1.1 S \sqrt{\pi \frac{a}{Q}} \tag{1}$$

where K_{sf} is the stress-intensity factor corresponding to the surface flaw, S is the applied stress, a is the size of the flaw, and Q is the shape factor.

Additionally, some other important factors must be considered for the pit-to-crack transition, such as loading conditions, the strain generated, solution corrosiveness, the toughness and microstructure of the material.[22,26,27]

The reason why many cracks initiate at the bottom of the pits is a high stress concentration at the more narrow area of a pit, which generally corresponds to the bottom of the pit. This assumption was well demonstrated with a corrosion-fatigue model made by Kondo:[28,29]

$$\Delta K_{\mathrm{fs}} = 2.24 \sigma_{\mathrm{a}} \sqrt{\pi c \frac{a}{Q}} \tag{2}$$

where σ_{a} is the stress amplitude, α is *a/c, 2c* is the flaw size, a is the pit depth, and Q is the shape factor. This formula clearly shows that the stress-concentration factor may increase significantly with the pitting depth.

The increase in the pitting depth was not the only factor causing the crack initiation. If the corrosion rate is high, only dissolution will occur and cracks will not develop. SEM observations revealed that although some pits were greater and deeper than the others, no crack was initiated from these pits. Their initiation depends on the microstructure and the equilibrium between the dissolution rate and different stress concentrations.

The determination of the critical pit size needed for the transition from pitting to cracks was developed by Shi et al.[30] They established that the nucleation of cracks is controlled by the competition between the processes of pit growing (dissolution) and crack growing (stresses due to a plastic deformation).

4 CONCLUSIONS

The investigation carried out in this work analyzed the physicochemical effects of two typical soils common in Mexico when in contact with the X52 pipeline steel. The value of the SCC index, which is <0.8 (RAR, TFR, PER, ELR and εR) indicates that the X52 pipeline steel may be slightly susceptible to SCC only in the saturated calcareous soil, which was corroborated by the secondary cracks in the gage section. Most of the cracks detected in the specimens of the X52 steel exposed to the saturated calcareous soil were found at the bottom of the pits. The location of the cracks in the pits may be related to the stress intensification at this place. Continuous loading during the SSRT produced a microstrain at the bottom of a pit, facilitating the pit-to-crack transition. The morphological factor and critical pit size were combined with the stresses, enhancing the transition from pitting to cracks. For the specimens metallographically prepared, the maximum cracking velocity of 6.76 mm/year was obtained. This cracking velocity is only an assumption as the time, at which the cracks actually start in a specimen during an SSR test, is unknown.

5 REFERENCES

[1] P. Cazenave, S. Tandon, M. Gao, R. Krishnamurthy, R. Peverelli, C. Moreno, E. Díaz, Assessment and management of SCC in a liquid pipeline: case study, Proceedings of the 8th International Pipeline Conference (IPC), ASME, Calgary, Alberta, Canada, **2010**, doi:10.1115/IPC2010-31140

[2] D. J. Kong, Y. Z. Wu, D. Long, Stress corrosion of X80 pipeline steel welded joints by slow strain test in NACE H_2S solutions, J Iron Steel Res Int, 20 (**2013**), 40–46, doi:10.1016/S1006-706X(13)60042-4

[3] M. Monnota, R. P. Nogueira, V. Roche, G. Berthomé, E. Chauveau, R. Estevez, M. Mantel, Sulfide stress corrosion study of a super martensitic stainless steel in H_2S sour environments: Metallic sulfides formation and hydrogen embrittlement, Applied Surface Science, 394 (**2017**), 132–141, doi:10.1016/j.apsusc.2016.10.072

[4] Z. Fan, X. Hu, J. Liu, H. Li, J. Fu, Stress corrosion cracking of L360NS pipeline steel in sulfur environment, Petroleum, 3 (**2017**), 377–383, doi:10.1016/j.petlm.2017.03.006

[5] O. I. Zvirko, S. F. Savula, V. M. Tsependa, G. Gabetta, H. M. Nykyforchyn, Stress corrosion cracking of gas pipeline steels of different strength, Procedia Structural Integrity, 2 (**2016**), 509–516, doi:10.1016/j.prostr.2016.06.066

[6] V. A. Voloshyn, O. I. Zvirko, P. Ya. Sydor, Influence of the compositions of neutral soil media on the corrosion cracking of pipe steel, Mater Sci, 50 (**2015**), 671–675 doi:10.1007/s11003-015-9770-7

[7] A. Benmoussat, M. Hadjel, Corrosion behaviour of low carbon line pipe steel in soil environment, J Corros Sci Eng, 7 (**2005**), 1–14, doi:10.18321/ectj626

[8] B. N. Leis, R. J. Eiber, Stress-corrosion cracking on gas-transmission pipelines: history, causes, and mitigation, Proceedings of the First International Business Conference on Onshore Pipelines, Berlin, 1997, http://igs.nigc.ir/STANDS/ARTIC/CP-50.PDF, 01.09.2018

[9] G. Van Boven, W. Chen, R. Rogge, The role of residual stress in neutral pH stress corrosion cracking of pipeline steels. Part I: Pitting and cracking occurrence, Acta Materialia, 55 (**2007**), 29–42, doi:10.1016/j.actamat.2006.08.037

[10] A. Eslami, R. Eadie, W. Chen, Effect of oxygen on near-neutral pH stress corrosion crack initiation under a simulated tape coating disbondment, Canadian Metallurgical Quarterly, 55 (**2016**), 177–185, doi:10.1080/00084433.2016.1180275

[11] W. Chen, R. Kania, R. Worthingham, G. Van Boven, Transgranular crack growth in the pipeline steels exposed to near-neutral pH soil aqueous solutions: The role of hydrogen, Acta Materialia, 57 (**2009**), 6200–6214, doi:10.1016/j.actamat.2009.08.047

[12] NACE TM-0198:2016 Slow Strain Rate Test Method for Screening Corrosion-Resistant Alloys (CRAs) for Stress Corrosion Cracking in Sour Oilfield Service, NACE International, Houston, Texas

[13] ASTM G-129:2013 Slow strain rate testing to evaluate the susceptibility of metallic materials to environmentally assisted cracking, ASTM International, West Conshohocken

[14] H. Asahi, T. Kushida, M. Kimura, H. Fukai, S. Okano, Role of microstructures on stress corrosion cracking of pipeline steels in carbonate-bicarbonate solution, Corrosion, 55 (**1999**), 644–652, doi:10.5006/1.3284018

[15] J. G. Gonzalez-Rodriguez, M. Casales, V. M. Salinas-Bravo, J. L. Albarran, L. Martinez, Effect of microstructure on the stress corrosion cracking of X-80 pipeline steel in diluted sodium bicarbonate solutions, Corrosion, 58 (**2002**), 584–590, doi:10.5006/1.3277649

[16] Z. Y. Liu, X. G. Li, C. W. Du, L. Lu, Y. R. Zhang, Y. F. Cheng, Effect of inclusions on initiation of stress corrosion cracks in X70 pipeline steel in an acidic soil environment, Corros Sci, 51 (**2009**), 895–900, doi:10.1016/j.corsci.2009.01.007

[17] M. A. Arafin, J. A. Szpunar, Effect of bainitic microstructure on the susceptibility of pipeline steels to hydrogen induced cracking, Mat Sci Eng A-Struct, 528 (**2011**), 4927–4940, doi:10.1016/j.msea.2011.03.036

[18] M. Sawamura, H. Asahi, T. Omura, H. Kishikawa, N. Ishikawa, M. Kimura, Near neutral pH SCC properties of pipeline steels of grade X80 and X52, Corrosion, Paper No. 11286 (**2011**), https://www.onepetro.org/download/conference-paper/NACE-11286?id=conference-paper%2FNACE-11286, 01.09.2018

[19] N. U. Terzi, M. Ü. Özsoy, F. Yilmaztürk, B. Güllü, C. Erenson, Effects of tire chips on the shrinkage and cracking characteristics of clayed soils, Mater. Tehnol., 52 (**2018**) 2, 143–150, doi:10.17222/mit.2017.057

[20] P. Maruschak, V. Gliha, I. Konovalenko, T. Vuherer, S. Panin, Physical regularities in the cracking of nanocoatings and a method for an automated determination of the crack-network parameters, Mater. Tehnol., 46 (**2012**) 5, 525–529

[21] B. Zorc, M. Imamovi, L. Kosec, B. Kosec, A. Nagode, Influence of non-metallic inclusions on the formation of hot cracks in the weld and HAZ, Mater. Tehnol., 48 (**2014**) 1, 149–154

[22] B. Y. Fang, R. L. Eadie, W. X. Chen, M. Elboujdaini, Pit to crack transition in X-52 pipeline steel in near neutral pH environment Part 1 – formation of blunt cracks from pits under cyclic loading, Corros Eng Sci Techn, 45 (**2010**), 302–312, doi:10.1179/147842208X386304

[23] S. Seitl, P. Huta, Fatigue-crack propagation near a threshold region in the framework of two parameter fracture mechanics, Mater. Tehnol., 41 (**2007**) 3, 135–138

[24] A. Lee-Sak, P. Yeun-Chul, K. Ho-Kyung, A numerical study of the tensile stress concentration in a hemi-ellipsoidal corrosion pit on a plate, International Journal of Steel Structures, (**2018**), 1–13, doi:10.1007/s13296-018-0134-7

[25] Ch. Evans, R. Leiva-Garcia, R. Akid, Strain evolution around corrosion pits under fatigue loading, Theoretical and Applied Fracture Mechanics, 95 (**2018**), 253–260, doi:10.1016/j.tafmec.2018.02.015

[26] D. Hoeppner, A. Taylor, Chapter 13 – Modeling pitting corrosion fatigue: pit growth and pit-crack transition issues, 2012, https://www.researchgate.net/profile/David_Hoeppner/publication/267221234.pdf, 01.09.2018

[27] A. Turnbull, D. A. Horner, B. J. Connolly, Challenges in modelling the evolution of stress corrosion cracks from pits, Engineering Fracture Mechanics, 76 (**2009**), 633–640, doi:10.1016/j.engfracmech.2008.09.004

[28] Y. Kondo, Prediction of fatigue crack initiation life based on pit growth, Corrosion, 45 (**1989**), 7–11, doi:10.5006/1.3577891

[29] T. Zhao, Z. Liu, C. Du, Ch. Liu, X. Xu, X. Li, Modeling for corrosion fatigue crack initiation life based on corrosion kinetics and equivalent initial flaw size theory, Corrosion Science, 142 (**2018**), 277–283, doi:10.1016/j.corsci.2018.07.031

[30] P. Shi, S. Mahadevan, Damage tolerance approach for probabilistic pitting corrosion fatigue life prediction, Eng Fract Mech, 68 (**2001**), 1493–1507, doi:10.1016/S0013-7944(01)00041-8